



# Automated lab-on-chip for the specific detection of invasive species through environmental DNA

Monisha Elumalai<sup>a,b,c</sup>, Andrey Ipatov<sup>a</sup>, Joana Guerreiro<sup>a,d,e,f,\*</sup>, Marta Prado<sup>a,g</sup>

<sup>a</sup> Food Quality and Safety Research Group, International Iberian Nanotechnology Laboratory, Portugal

<sup>b</sup> Vigo University, Chemistry, Spain

<sup>c</sup> Weldon School of Biomedical Engineering, Purdue University, USA

<sup>d</sup> BioMark@ISEP, School of Engineering of the Polytechnic Institute of Porto, Portugal

<sup>e</sup> CEB/LABBELS, Center of Biological Engineering, Minho University, Campus de Gualtar, Portugal

<sup>f</sup> CIETI-LabRISE, School of Engineering, Polytechnic Institute, 4249-015 Porto, Portugal

<sup>g</sup> Department of Analytical Chemistry, Nutrition and Food Science, Food Technology Division, School of Veterinary Sciences, University of Santiago de Compostela, Lugo, Spain

## ARTICLE INFO

### Keywords:

Plasmon coupling  
Signal amplification  
DNA sensing  
Nanoparticles  
Color sensor  
Automated detection

## ABSTRACT

The ability to detect nucleic acid sequences is revolutionizing the fast identification of specific organisms, particularly with Lab-on-a-chip systems. However, these often rely on complex processes, skilled personnel, and external control devices which limits automation. To address this, we present an automated, portable, and easy-to-fabricate lab-on-chip that combines enzyme-assisted DNA signal amplification and optical detection for in-situ monitoring of zebra mussel invasive species in the environment. Zebra mussels DNA triggers enzyme-assisted signal amplification through hybridization, leading to a quantitative colorimetric response. The sensing performance exhibited enhanced sensitivity when increasing AuNPs diameter from  $23.3 \pm 1.6$  to  $67.4 \pm 2.0$  nm. Quantitative colorimetric approaches displayed an LoD of 0.5 pM, 19-fold increase in sensitivity when compared to naked eye. The system enabled to discriminate single nucleotide polymorphism (SNP) for concentrations from 130 pM and to successfully analyse Zebra mussel samples from the Guadalquivir River. Experiments were conducted by the user and an automated device. The accuracy was tested with a 60 pM sample which was pre-treated externally and analysed by the automated system resulting in relative error of 16.8% and 13.4%, respectively. The automated system reduced the analysis time by 1 h and 20 min, great advantage for *in-situ* analysis.

## 1. Introduction

Invasive alien species (IAS) are non-native species deliberately or accidentally introduced outside their natural habitat by human action, posing a real threat to biodiversity, human health, or the economy[1]. This is one of the main causes of biodiversity loss, since IAS may outcompete native species, act as predators, and/or spread diseases, harming the environment, and compromising the life of native species [2]. The concept of chip-based devices (e.g. lab-on-chip) as monitoring systems has gained significant importance due to their portability, allowing for rapid and *on-site* analysis, cost-effectiveness, and ease of use [3–5]. These devices are typically based on microfluidic systems and have been used in a wide range of applications[6,7]. Microfluidic devices have evolved from costly and timely fabrication devices to

alternative microfluidic system prototypes produced using the polymeric material polydimethylsiloxane (PDMS), through moulds created by wax printing, xurography, or polymethyl methacrylate (PMMA) computer numerical control (CNC) machining. These approaches circumvent the requirement for numerous fabrication stages, highly trained personnel, and costly cleanroom facilities[8–10]. Chip-based microfluidic technology shifted the paradigm of standard laboratory procedures by facilitating the execution of a diverse range of operations on a single chip. Several efforts have been made to transform the conventional molecular-based methods for DNA amplification such as the gold standard Polymerase Chain Reaction (PCR), or alternative enzyme-based approaches for DNA/nucleic acids detection[11]. Microfluidic technology has also been applied to isothermal amplification techniques such as LAMP[12], Recombinase polymerase

\* Corresponding author at: CEB/LABBELS, Center of Biological Engineering, Minho University, Campus de Gualtar, Portugal.

E-mail address: [joanarguerreiro@gmail.com](mailto:joanarguerreiro@gmail.com) (J. Guerreiro).

<https://doi.org/10.1016/j.snb.2023.134722>

Received 1 August 2023; Received in revised form 29 September 2023; Accepted 3 October 2023

Available online 5 October 2023

0925-4005/© 2023 Elsevier B.V. All rights reserved.

amplification (RPA)[13], among others, which operate at a constant temperature and therefore miniaturization is greatly simplified by not requiring a thermal cycling process[14]. Despite the advantages of these molecular-based methods, novel alternatives to DNA amplification have arisen, offering interesting advantages. Among these alternatives are the signal-based amplification methods, which have been developed to attain ultrasensitive detection by enhancing the detectable signal. One of these methods is Nicking endonuclease-assisted signal amplification, an enzyme-based signal-based amplification technique. In this approach, the nicking endonuclease (NEase) recognizes and cleaves a specific site of one strand of the double-stranded DNA (dsDNA) while keeping the other strand (target) intact for the next cleavage cycle, resulting in signal amplification.

The combination of DNA-based methods with gold nanoparticles (NPs) has also revolutionized the molecular field and its optical detection, contributing to colorimetric detection and sensitivity enhancement. Gold NPs (AuNPs) are prominently used in colorimetric biosensing due to their unique intrinsic optical properties with high extinction coefficients and can be used as transducers. One of the optical properties of AuNP extensively explored in biosensors is their aggregation, which causes a coupling of the AuNP plasma modes, inducing a red shift and broadening of the longitudinal plasma, observed by naked eye. The localized surface plasmon resonance (LSPR) coupling of AuNPs depends on the size, shape, and interparticle distance between AuNPs [15]. Signal amplification methods based on AuNP for the colorimetric detection of DNA have been successfully applied [16–20]. Although this approach enables simple naked eye detection, their accurate and precise detection often requires a spectrophotometer or an optical fiber. Smartphones have gained attention as a detection tool due to their availability and simplicity, enabling them to overcome subjectivity associated with the detection by naked eye. Likewise using the smartphone for RGB color analysis and quantification results in higher accuracy. The effective and successful RGB analysis for the quantification of glucose in urine samples[21], detection of mercury(II) ions in water samples[22], and even the fast assessment of pathogenic bacteria [23] have been reported in the literature.

Several fully integrated microfluidic devices have been developed including multiple tasks such as DNA extraction, amplification, and optical detection on a single platform. Oh et al. described a fully automated colorimetric system for foodborne pathogen detection using an integrated centrifugal microfluidic device. Even though centrifugal microfluidics enables the combination of multiple steps in a single chip, the disc-shaped micropattern is complex and usually requires custom-made centrifugal systems for rotational speed control[12]. Considering the need for multiple sample analysis some platforms have been described such as an automated microfluidic system based on soft lithography of PDMS for high sample throughput developed by Kim et al.[24]. Some of these platforms are based on colorimetric detection which might introduce detection ambiguity. To fulfil that gap, the combination of smartphones or optical fibers to replace bulky equipment, and obtain accurate colorimetric detection of nucleic acids has been proposed [23],[25]. Nevertheless, the need to minimize the complexity of microfluidic devices while integrating multiple steps into a singular device, all while maintaining the capability of conducting high-throughput analysis of multiple samples is a long-sought requirement. Additionally, applications such as *in-situ* environment monitoring of invasive species require DNA-based sensors designed to rapidly distinguish between closely related organisms.

Here we present an automated, portable, fast, sensitive, and easy-to-fabricate lab-on-chip microfluidic system that integrates 5 flow channels to perform signal-based amplification of 5 samples simultaneously. The holder where the cartridge is assembled integrates two Peltier creating two distinct heating regions, for lower (58 and 37°C) and higher (80°C) temperatures. The hybridization and nicking enzyme activity are favoured at 58 and 37°C, respectively, while at 80°C the deactivation of the nicking enzyme occurs, enabling the amplification reaction inside the

channels. The cartridge has also a channel in the middle with a central reservoir to where the samples are sequentially sent for the colorimetric reading, enabling the early monitoring of the invasive species *Dreissena polymorpha* (zebra mussel) in the environment. The detection principle relies on signal amplification via nicking enzyme activity on the target DNA sequence, combined with an optical/colorimetric signal that offered improved sensitivity. The disposable microfluidic chip is connected to a portable multi-setup that automatically runs according to pre-defined user commands. The system also integrates enzyme-assisted signal amplification, and colorimetric DNA detection through a miniaturized optical sensor, enabling automated and timely analysis.

## 2. Materials and methods

### 2.1. Materials and reagents

All DNA sequences, including the thiol modified at 3' and 5' end were purchased from Stabvida (Caparica, Portugal) and prepared in autoclaved pyrogen, DNase, RNase free ultrapure water (MQ). Nicking endonuclease enzyme Nt. *AlwI* (NEase) and buffer was purchased from New England Biolabs (Ipswich, MA, USA). Genomic DNA clean up kit and DNeasy PowerSoil Pro Kit were purchased from MACHEREY-NAGEL and Qiagen (Barcelona, Spain), respectively. All chemicals were of molecular biology grade and purchased from Sigma-Aldrich (Sigma-Aldrich, St. Louis, MO, USA). The buffers used were: 0.1 M phosphate buffer pH 7.0 (PB), 80 mM citrate buffer pH 3 (CB), salting buffer corresponds to the buffer used for salt aging DNA loading method composed of 2 M NaCl, 0.01% sodium dodecyl sulfate – SDS - in 10 mM phosphate buffer (SB), hybridization buffer composed by 2 M NaCl in 10 mM phosphate buffer (HB). All the pH adjustments were carried out with NaOH or HCl.

### 2.2. DNA sequence selection

The target DNA is a sequence from an invasive species, *Dreissena polymorpha*, commonly known as Zebra Mussel. DNA design and selection (detailed in [Supplementary Information](#)) were performed as previously reported [16].

### 2.3. Synthesis of gold nanospheres (AuNP), characterization, and DNA loading

The synthesis of AuNP followed the method described by Brown et al. [26]. Synthesis details of large-size citrate-capped AuNPs in an aqueous medium as well as the stabilization conditions for the synthesized AuNPs are presented in the [Supplementary Information](#). In this work, two batches were synthesized. Batch 1 was mainly used for optimizing parameters for nicking enzyme amplification and colorimetric detection while batch 2 was used for testing the amplification and colorimetric detection within the microfluidic system (batch 2 was required due to insufficient volume of batch 1 to run further experiments). AuNPs were characterized by UV-vis spectrophotometer, Transmission Electron Microscope (TEM), and Dynamic Light Scattering (DLS). Details of sample preparation for characterization are presented in the [Supplementary Information](#).

AuNPs were loaded with two different DNA sequences performed through salt-aging method. The detailed protocols are described in the [Supplementary Information](#).

### 2.4. Microfluidic chip design and fabrication

The disposable microfluidic cartridge (microfluidic chip) made of PDMS was fabricated using a mould of polymethyl methacrylate (PMMA) milled with a CNC Machine (High Speed Milling System, FlexiCam Viper, Germany). The mould's design was developed using the ArtCam Jewelsmith Software (Autodesk), which allows visualizing the

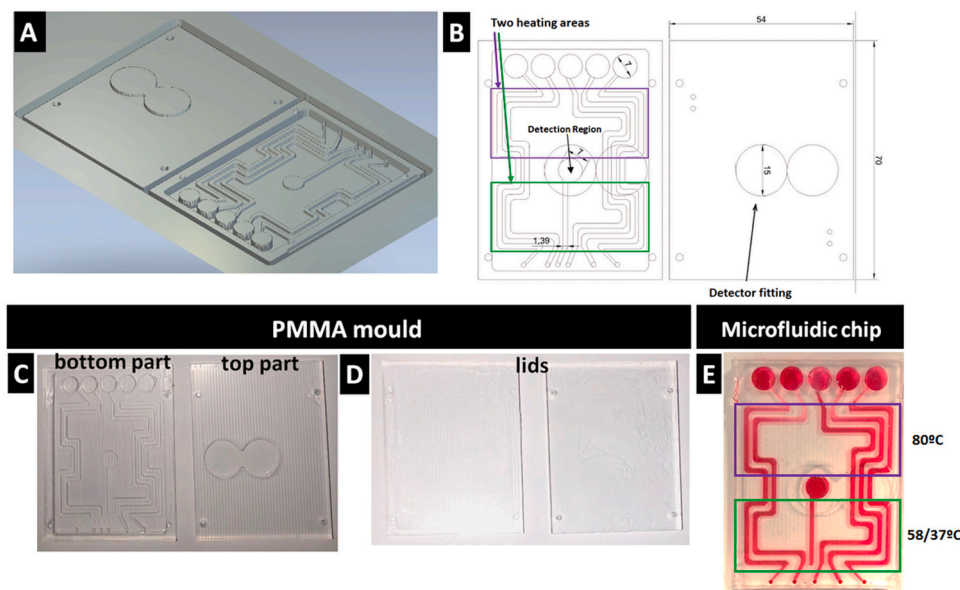


**Fig. 1.** Different steps for the disposable microfluidic chip design and fabrication. A) chip in 3D view, the two cylindrical openings on the left are the areas where the colorimetric sensor is placed, B) chip 2D drawing, C) PMMA moulds, D) PMMA lids, E) disposable microfluidic chip.

3D cutting based on the 2D drawing, minimizing fabrication errors, as shown in Fig. 1A and B. The PMMA mould consists of two parts: the bottom part with inversed patterned channels and chambers, and the top part with a patterned circular reservoir in the center, as shown in Fig. 1C. For each part of the mould, a flat lid was also fabricated (0.5 mm thickness), Fig. 1D. The mould was fabricated within 2 h, and before its use was thoroughly rinsed with ethanol, MQ, and dried.

The PDMS was prepared by mixing the curing agent and PDMS monomers, in a 1:10 ratio, followed by 30 min in vacuum to promote degassing. The preparation of one disposable cartridge requires approximately 10 g of PDMS. The liquid PDMS was poured into the two parts of the mould, which were clipped together with a flat lid and placed in an oven for 2 h at 65 °C. The two parts of cured PDMS were removed from the moulds and bonded together using Harrick plasma cleaner PDL-002-CE (oxygen atmosphere, 800 torr, 50 W of RF, and 2 min), and kept in an oven at 65 °C for 30 min, clamped with clips. The microfluidic chip was fabricated with the dimensions of 70 (L) × 54 (W) × 5 mm (thickness).

The disposable microfluidic cartridge, Fig. 1E, features 5 flow channels of 0.75 × 1.5 × 0.9 mm (H×W×L), fitting a total volume of 100 µL each, and formed after bonding the top and bottom PDMS parts. At the end of each channel, a cylindrical well of 100 µL was used for sample storage when the temperature of the system was readjusted. The channel in the middle of the chip with the dimensions of 0.75 × 1.39 mm (H×W) had a cylindrical reservoir of 7 mm diameter, detection region, to where the sample was sent for colorimetric read-outs. The cylindrical reservoir with a small opening for air purge could be filled with up to 20 µL. This central region was aligned in parallel with the colorimetric sensor placed on top of the cartridge. The total thickness of the disposable microfluidic chip was 5 mm.

The fabricated cartridge displays 5 independent flow channels that allow the simultaneous signal amplification of 5 different samples. For the calibration of the system, increasing DNA target concentrations were tested. Each DNA target concentration was injected, in the respective flow channel, where the samples were moved to the first temperature region (58 °C) for 5 min, then to the well at the end of each channel until that region reaches the 37 °C before moving back the sample that remains for 120 min and only then to the second region at 80 °C. After the amplification step in each channel, the samples were sequentially redirected to the central colorimetric detection region for the

colorimetric analysis by the colour sensor. To avoid contamination, the channel with the detection region (Port P4) was cleaned by flushing MQ water.

## 2.5. System components

The system is composed of a syringe pump (FIALab Company, USA), a multi-position valve with 10 ports, and a homemade temperature controller assembled, which communicates with the software through Arduino hardware. The Flora Color Sensor with white illumination LED - TCS34725 (Adafruit), Fig. 2, incorporates a white LED for sample illumination and three filters on the detector (red, green, and blue) enabling the signal to be decomposed into three components (RGB).

The homemade controller contains a software PID program and hardware driver (Dual MC33926 Motor Driver, Pololu) with the possibility to change output polarity. This controller holds the temperature with a precision of 1 °C and a high current limit (3 A) enabling fast temperature changes. As a heating/cooling unit, two Peltier elements with 20 × 40 mm<sup>2</sup> dimensions were used.

The communication between the software and the pump, position valves, color sensor, and temperature controller was carried out by one single Arduino Mega through serial ports.

The assembly of all these components enables the temperature sensor to control temperatures required for enzyme amplification directly inside the cartridge, the pump to move the sample back and forward from the sample microtube to the cartridge at a specific flow rate, as well as promote the mixing, and the color sensor to illuminate the sample and collect the RGB signal. The setup integrates two pieces of small size that can be easily transported. However, small adjustments could be made to integrate them into a single piece.

## 2.6. Automated analysis

The control of all the components was conducted by the developed software using a C++ programming language. The software allows manual instruction to the system or sequential order of commands can be created for automated control (Fig. S11 SI example of sequential order of commands for the amplification and colour readout (probe and target hybridization, followed by nicking endonuclease activation/inactivation and AuNP addition for colorimetric detection). A scheme of

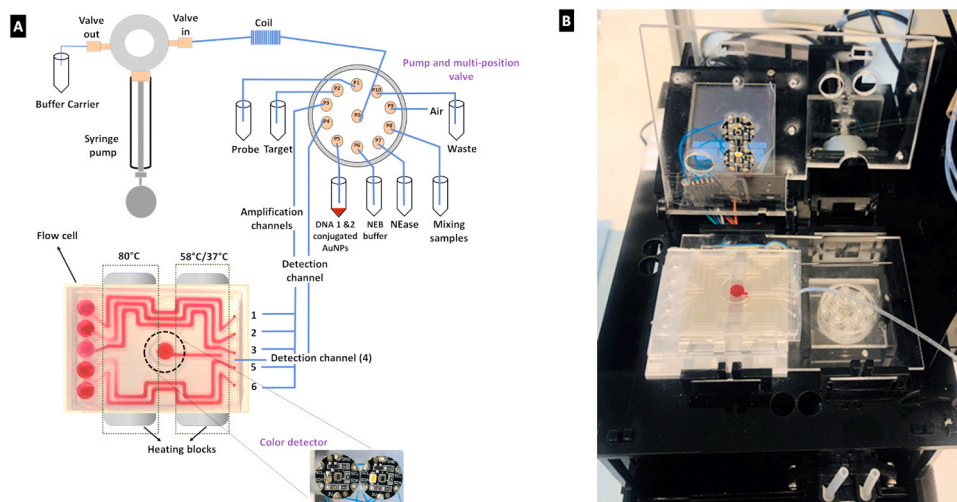


**Fig. 2.** Portable system with an integrated disposable microfluidic cartridge **A)** Detection schemes with an integrated syringe pump, multi-position valve and flow cell, color sensor, home-made temperature controller, and software user interface, **B)** The Flora Color Sensor with white illumination LED - TCS34725 (Adafruit) was assembled in a lid piece that when closed is parallel to the detection region of the microfluidic cartridge.

the whole system and the user interface are displayed in Fig. 2. After sending the commands to the controller, the system could run without being connected to a laptop.

### 2.7. Optical detection testing inside the cartridge

Two approaches were tested at this stage 1) the preparation of the reaction mixture for signal amplification outside the cartridge and only the RGB reading taken inside the microfluidic system; and 2) both steps, signal amplification and colorimetric detection, inside the disposable microfluidic chip. Standard tubes of 0.762 mm inner diameter were used for solution injection into the system.

In the first approach, 20  $\mu\text{L}$  containing 10  $\mu\text{L}$  of the reaction mixture and 10  $\mu\text{L}$  of nanoparticle (NP) mixture were mixed outside and then introduced in the microfluidic system for RGB readings. In the second approach the sample preparation, amplification, and colorimetric detection were done within the microfluidic system by assigning a sample/solution to each port. To perform the calibrations, the solutions placed at each port were: P1-Probe 4  $\mu\text{L}$  (0.065  $\mu\text{M}$ ), P2 - Target 4  $\mu\text{L}$  (0.065  $\mu\text{M}$ ), P3 - Channel 1 of PDMS chip, P4 - optical detection region in PDMS chip, P5-10  $\mu\text{L}$  of NP mixture containing AuNP loaded with DNA 1 and 2 (0.017 nM each), PB (3.5 mM) and HB buffer containing NaCl (0.1 M) and PB (0.5 mM), P6-NEB (10  $\times$ ), P7- NEase 100 units, P8-sample mixing microtube, P9-air, and P10- waste. The automated system with times and volumes followed the steps indicated in Table 1.

### 2.8. RGB data collection and analysis

Two approaches were used to obtain the RGB coordinates, a digital photo collected with a smartphone and a direct measurement with a color sensor. Further details about the photos captured and their environment are described in SI. The RGB analysis based on a photo was done by collecting the three-color coordinates Red (R), Green (G), and Blue (B) values using a spot size on the region corresponding to an average of 104 total pixel counts to each sample through Image J software. The software provides an average of RGB for each spot size, a total of 3 images were analysed, and the RGB average was considered. The R/B data were normalized by dividing these data by the ratio obtained for the “only NEase” control. The normalized R/B ratio was then plotted against increasing concentrations of DNA target. The curve was fitted with the Origin 9 software logistic function. The R/B ratio of tested samples was based on 3 images.

The RGB values obtained digitally with the automated system were

**Table 1**

User's recipe with general commands for the automated analysis using the microfluidic system.

Steps	Protocol
	The temperature was set to 58 $^{\circ}\text{C}$
Step 0	Fill the syringe pump and the whole system including the mixing coil with the carrier buffer.
Step 1	Fill the tubes connecting the ports with mixing coil with the carrier buffer.
Step 2	The amplification protocol was initiated by the sequential aspiration, at the flow rate of 10 $\mu\text{L/s}$ , into the mixing coil of 5 $\mu\text{L}$ of NEB (P6), 4 $\mu\text{L}$ probe (P1), and 4 $\mu\text{L}$ target (P2). These volumes were physically separated from the carrier buffer by 10 $\mu\text{L}$ of air at each end.
Step 3	The volumes of NEB, probe and target were dispensed into a microtube to promote further mixing and injected into the first region of the cartridge (P3, channel 1 -Fig. 1E). To reach that region, 60 $\mu\text{L}$ of the carrier was injected.
Step 4	The solution remained in that region for 300 s at 58 $^{\circ}\text{C}$ , favouring hybridization.
Step 5	This solution was then retrieved from the cartridge, mixed with 10 $\mu\text{L}$ of NEase (P7) in the mixing Eppendorf (P8), and sent back to the first region (P3, channel 1) of the cartridge now at 37 $^{\circ}\text{C}$ to activate the NEase during 7200 s total.
Step 6	After that, the mixture was pushed to the second region of the cartridge (P3, channel 1), already set at 80 $^{\circ}\text{C}$ to inactivate Nease. The solution remained in the zone for 1500 s
Step 7	At the end of each channel of the cartridge a 100 $\mu\text{L}$ reservoir was used to store the reaction mixture when heating was not required.
Step 8	The 10 $\mu\text{L}$ reaction mixture was then retrieved and mixed at P8 with 10 $\mu\text{L}$ of AuNP loaded with DNA 1 and 2.
Step 9	The mixture was sent to the central detection reservoir for signal readout collected over 1800 s

recorded every 2.15 s for 30 min and the last 10–15 min were averaged (stable colorimetric response observed). This R/B data were also normalized as previously described by dividing these data by the ratio obtained for the “only NEase” control. The R/B ratio was then calculated and plotted against increasing target DNA concentrations.

### 2.9. Preliminary assays for nicking enzyme amplification and colorimetric detection

For the nicking enzyme assisted signal amplification we followed our previously reported protocol [16]. Briefly, the reaction mixture containing both DNA probe and target were prepared and placed in a thermomixer at 58  $^{\circ}\text{C}$  for 5 min for duplex formation. Then, NEase was added and incubated at 37  $^{\circ}\text{C}$  for 2 h and at 80  $^{\circ}\text{C}$  for 20 min to

deactivate Nease. For the colorimetric detection, part of this mixture was mixed with AuNP modified with DNA1 and DNA2 [20]. The colorimetric response is obtained within 30 min. Further details are described in the [Supporting Information](#).

### 2.10. Evaluation of real matrices effect and real sample analysis in a lab setting

The matrix effect was tested with river water non-contaminated by DNA from *D. polymorpha*. The procedure for nicking enzyme amplification and colorimetric detection was repeated in *D. polymorpha* free river water spiked with target DNA with increasing target concentrations ranging from 376 pM to 1 pM.

Competitive assays were also conducted by preparing samples with both target and mismatched sequences, for testing the colorimetric system capability to specifically identify the target sequence in river water. The river water non-contaminated with zebra mussel was filtered with a pore size 0.2  $\mu\text{m}$  syringe filter and purified with gDNA clean up kit. The test involves testing of match and mismatch DNA sequences individually (40 pM) as well as target and mismatch proportion concentrations (pM) of 40:40, 32:40, 25:40, 16:40, 8:40, corresponding to the ratio of 0.2, 0.4, 0.6, 0.8, and 1.

Real samples were provided by Confederación Hidrográfica del Guadalquivir and they were collected from the Iznajar reservoir, in Spain (Guadalquivir River, Spain). Different environmental samples were obtained, the meat was extracted from two well identified zebra mussel samples as well as the shell for DNA detection, degraded zebra mussel meat (where specimens were stored for more than 2 months), water used to transport zebra mussel, and contaminated river water were tested using a colorimetric system using the non-contaminated river water as control. DNA extraction and purification of these samples was done for all samples.

## 3. Results and discussion

This work describes an easy-to-fabricate microfluidic chip that combines DNA signal amplification through nicking enzyme activity and accurate colour detection. The system allows simultaneous optical and colorimetric detection, facilitating the early monitoring of DNA from invasive species, in environmental samples. Additionally, this automated system enables faster analysis and user-free measurements due to pre-defined user commands. [Fig. 2](#) shows the integrated portable disposable microfluidic cartridge.

The detection system is based on plasmonic nanoparticles and monitors their aggregation which induces a colour change and enables the colorimetric detection of DNA targets. Considering that plasmon coupling (aggregation) sensitivity is mainly limited by the number of DNA sequences available to interact with their complementary strands at the NP's surface, an alternative to improve it, is by using large-size AuNP[27] since the size of the gold nanoparticles greatly influences the sensitivity of the system. The larger the AuNPs the higher the extinction coefficients are, resulting in a better optical signal, leading to improvement in the sensitivity of the detection system[28]. Large-size AuNPs (> 40 nm) have a higher extinction coefficient and their curvature decrease facilitates the bindings between the DNA target and complementary sequences (probe) to a certain extent. Additionally, the sensitivity enhancement is related to the increase in the AuNP size, which decreases the surface coverage of DNA sequences onto AuNPs where a smaller number of DNA sequences were required for better optical signal[29]. Thus, sensitivity limitations associated with small plasmonic nanoparticles can be improved by using larger size NP. Large AuNPs were synthesized and characterized by UV-vis, TEM, and DLS. Their characterization showed an LSPR peak at 538.9 nm using UV-vis and a size of  $67.4 \pm 2.0$  nm using TEM. Characterization details are described in the Characterization section of the [SI](#) and, data is shown in [Fig. S1](#). Prior AuNP preconcentration, three concentrations of sodium

citrate of 1, 3, and 10 mM were tested to assess AuNP stabilization. The concentration of 3 mM sodium citrate was selected as it avoided aggregation, as seen in [Fig. S2](#). The AuNP were loaded with DNA 1 and 2 sequences, through the salt-aging method, creating two distinct sets of AuNP to be further used, as shown in [Fig. S3](#). Their characterization and colorimetric optimizations are detailed in the [SI](#) and [Fig. S4-S9](#). In these optimizations included the comparison of sensing performance with smaller and larger AuNP ( $23.3 \pm 1.6$  nm versus  $67.4 \pm 2.0$  nm) was evaluated. The data shown in [Fig. S8](#), showed enhanced sensitivity when using larger AuNPs. Thus, the following tests were carried out with NPs of  $67.4 \pm 2.0$  nm.

### 3.1. Optical performance using the microfluidic cartridge

The colorimetric detection of Zebra Mussel DNA is based on the NE amplification reaction. Thus, the sensitivity and selectivity of the system were optimized regarding AuNP, DNA probe, DNA target concentrations, the effect of river waters samples, as well as the comparison of naked eye detection and RGB analysis outside the microfluidic system as detailed in [SI Fig. S9](#).

The measurements carried out inside the microfluidic disposable cartridge using the automated portable setup were already tested with the optimized conditions.

The automated and disposable microfluidic cartridge was developed for *in-situ* analysis of eDNA from zebra mussel. The whole setup integrates a temperature module where the disposable microfluidic cartridge is placed, and a PMMA lid with the Flora Color Sensors in the central part that, when closed, becomes parallel and aligned with the central detection reservoir of the middle channel of the cartridge. To control the flow rates and fluid directions, a multi-position valve and a syringe pump were connected to the cartridge holes by tubing (PTFE, 1/16" (1.6 mm) OD  $\times$  0.2 mm ID, 20 M). The system was controlled by the software, which followed commands based on user-made recipes for automation of the measurements. The disposable microfluidic cartridge with 5 channels was designed to accommodate two distinct heating regions, for lower (58 and 37°C) and higher (80°C) temperatures, as indicated in [Fig. 2](#). These two regions enabled the activation/deactivation of the nicking enzyme during the amplification reaction. The mixing of the reaction solutions and each sample, for nicking enzyme-assisted signal amplification, was carried out in individual channels, while the colorimetric DNA detection was done in the channel with the central detection reservoir of the cartridge. The cartridge and detector setup is shown in [Fig. 3](#), the cartridge is positioned on the holder integrating the Peltier system and the closed lid places the colorimetric sensor parallel to the detection region.

Firstly, only the optical signal was evaluated within this microfluidic system. For that, the nicking endonuclease amplification was performed outside of the cartridge only then 10  $\mu\text{L}$  of each reaction mixture of NE and DNAs prepared was added to 10  $\mu\text{L}$  of loaded nanoparticles and injected into the detection reservoir region of the disposable cartridge using pump/valves to measure the colorimetric signal (one sample at a time). This approach allowed optimization of the time required to achieve stable colorimetric measurements, to compare the obtained RGB data with data from a smartphone, to evaluate the capability to detect single nucleotide polymorphism and to evaluate environmental samples. After these assessments, the fully automated colorimetric analysis including the nicking endonuclease amplification was performed within the disposable cartridge.

### 3.2. Stability and accuracy of optical readout

The stability and accuracy of the colorimetric readout were checked with a red dye and the "only nicking enzyme" control for 600 and 3600 s, respectively. The red dye showed a constant color readout data over the 600 s while the control showed some signal fluctuation in the first seconds and reached a stable signal after 250 s, as demonstrated in

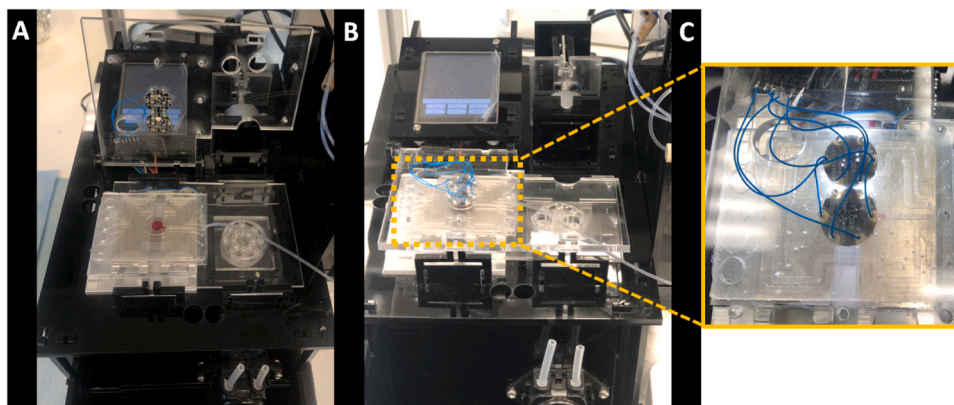


**Fig. 3.** Microfluidic setup and the lid incorporating the colorimetric sensor. A) cartridge positioned on the holder integrating the Peltier system, B) the closed lid places the colorimetric sensor parallel to the detection region of the cartridge and C) closed-view of the lid with the colorimetric sensor during detection process.

**Fig. S10** of SI. Therefore, for all the further analysis, the colorimetric data were acquired between 500 and 2000 s

### 3.3. Comparison of RGB data using a smartphone digital image versus color sensor

The evaluation of the RGB data obtained with the commercial RGB sensor inside the microfluidic system was carried out by injecting into the detection channel of the cartridge 20  $\mu\text{L}$  of the solutions, with increasing target concentration and AuNP immediately after its mixture, at a flow rate of 10  $\mu\text{L}/\text{sec}$ . In these assays, a new batch of large AuNP (batch 2) was used, although for comparison the final concentration of metallic gold was similar for all assays. The assays inside the microfluidic cartridge were carried out with AuNP stabilised with 0.1 M NaCl, and a probe concentration of 260 pM (Probe to nanoparticle ratio is 20). The target concentration tested ranged from 260 to 1 pM. For comparison, DNA detection was also assessed by the naked eye, and RGB was obtained by a smartphone digital image using image J software and using color sensor in the microfluidic system. As previously demonstrated, the naked eye can only detect color changes when the difference

between the reflected wavelengths, which fall into the visible region, is large enough. Thus, the achieved detection limit was 10 pM ( $5.60 \times 10^{10}$  copies). Regarding the RGB color analysis, the two methods used responded slightly differently. The threshold corresponding to the absence of target, aggregation, was  $0.9580 \pm 0.0003$  for the digital image analysis, and  $0.8580 \pm 0.0006$  for the commercial RGB sensor. Both calibration curves followed a sigmoidal non-linear fitting, Equation 1, and showed the curve parameters of  $A1 = 0.85546$ ,  $A2 = 0.98493$ ,  $x0 = 2.3257$  and  $p = 1.16954$  for the digital image, and  $A1 = 0.95767$ ,  $A2 = 0.98659$ ,  $x0 = 21.96697$  and  $p = 0.51014$  for RGB sensor. Three calibration sets were obtained from 3 digital images showing consistent and stable color responses as shown in **Fig. 4**. The detection limit of digital image analysis showed a detection limit  $\sim 0.52$  pM ( $2.91 \times 10^9$  copies) while the RGB sensor was 0.59 pM ( $3.30 \times 10^9$  copies). Detection limits were calculated based on three times the standard deviation of the blank. The LoD obtained showed a 19-fold increase in sensitivity compared to naked eye detection limit. Thus, the RGB model demonstrated high accuracy and enhancement in sensitivity when compared to naked eye analysis.

RGB models have been widely used based on digital image

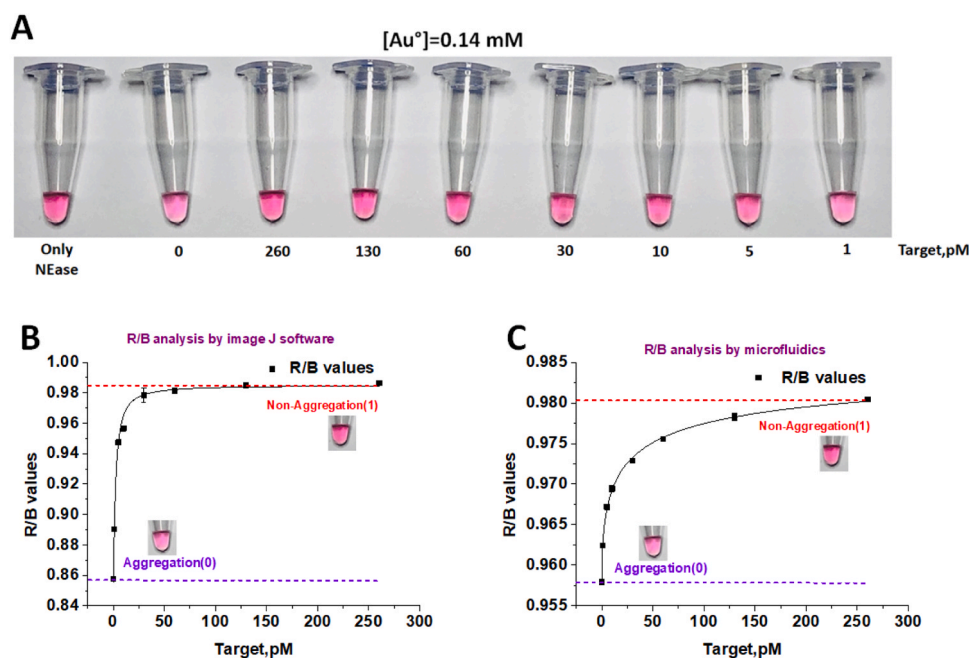


**Fig. 4.** Colorimetric response for increasing target concentrations by A) naked eye visualization, B) RGB coordinate analysis by ImageJ, and C) RGB data obtained by the optical sensor inside the microfluidic system.

information or directly acquired by commercial sensor devices, demonstrating the potential for several analytical applications [23,30]. Commercial RGB devices have also been integrated with technological advances in LED-based lighting, making them highly suitable for fast and accurate monitoring. Another great advantage of these commercial RGB sensors is their capacity for continuous and accurate monitoring.

### 3.4. Colorimetric detection of single nucleotide polymorphism

To evaluate the specificity of the developed method against close DNA sequences, the approach was challenged with a non-targeted sequence consisting on a DNA fragment including a single nucleotide variation at the 23rd nucleotide. Samples were prepared with this non-targeted DNA sequence with concentrations ranging from 260 to 0 pM and the colorimetric responses were compared by i) naked eye detection, ii) RGB color coordinate analysis by Image J software, and iii) microfluidic system color sensor. A slight aggregation appeared at the non-targeted DNA sequence concentration of 260 pM while full aggregation was clear from 130 pM, Fig. 5A. This indicates that only for the highest concentration, some extent of cross-reactivity from the non-targeted DNA sequence occurred. For all the other concentrations, the clear Au nanoparticle aggregation indicates that the presence of SNP do not induce a positive response, which means that contrary to what happens in the presence of target (no-aggregation) the system is able to discriminate non-targeted DNA sequence even with a single nucleotide mismatch. For the RGB data the curve parameters were  $A1 = 0.89992$ ,  $A2 = 1.0781$ ,  $x0 = 204.4$ , and  $p = 0.88455$  for digital image and  $A1 = 0.93701$ ,  $A2 = 1.02768$ ,  $x0 = 28.6$  and  $p = 0.23547$  for the commercial color sensor. Both RGB data displayed a signal change with increasing SNP concentrations towards a slight aggregation. The difference between the two RGB systems is that, with digital image analysis, the increasing of SNP concentration led to slower but continuous shift towards aggregation while for the color sensor this process was slower up to approximately 50 pM and faster below that concentration, as seen in Fig. 5B and C. This means that RGB systems have higher sensitivity than naked eye to distinguish the small colour effects induced by the non-targeted DNA sequence, although for RGB, no-aggregation

was only obtained for the highest non-targeted DNA sequence concentration, showing the ability to discriminate single nucleotide mismatch with high specificity [24,27,31].

### 3.5. Analysis of environmental samples on the microfluidic chip

The samples previously tested including DNA extract from zebra mussel specimens and river water containing zebra mussel were also tested with the color sensor integrated into the microfluidic system and in parallel analysed by naked eye, as shown in Fig. 6A. The environmental samples were monitored based on the calibration and the results displayed in Fig. 6B. The water contaminated with zebra mussel presented a concentration of  $713.9 \pm 12.2$  ( $0.0070 \pm 0.0030$  ng/ $\mu$ L), whereas the zebra mussel DNA extract showed a concentration higher than the standard solution of 260 pM concentration indicating that stock samples require dilution prior testing. The samples with only river water and only MQ water showed a pale red color, indicating aggregation, and were also below the detection limit of the system, as expected. The standard solution of 60 pM was tested to check the accuracy of the system, which showed a concentration of  $49.95 \pm 11.8$  pM ( $0.00049 \pm 0.00012$  ng/ $\mu$ L) with a relative error of 16.8% providing, therefore, a good approximation to the real concentration of the sample. Triplicates were made and for each sample, 139 RGB colour coordinates were average after reaching stable colorimetric readouts. As a reference, the total DNA concentration in ng/ $\mu$ L was estimated by Qubit fluorometer as described in Fig. 6B.

### 3.6. Automated analysis of the samples

The fully automated analysis of samples was conducted inside the microfluidic disposable cartridge, starting with the signal amplification process, and followed by colorimetric detection. The commands lines for the automatization were defined in a recipe described in Fig. S11 of SI and loaded into the software. Then, according to the user's recipe with instructions described in Table 1, the solutions were mixed and injected into the cartridge via ports in the pump and valve section. The syringe pump was filled with MQ water, which was used as the carrier. First, the

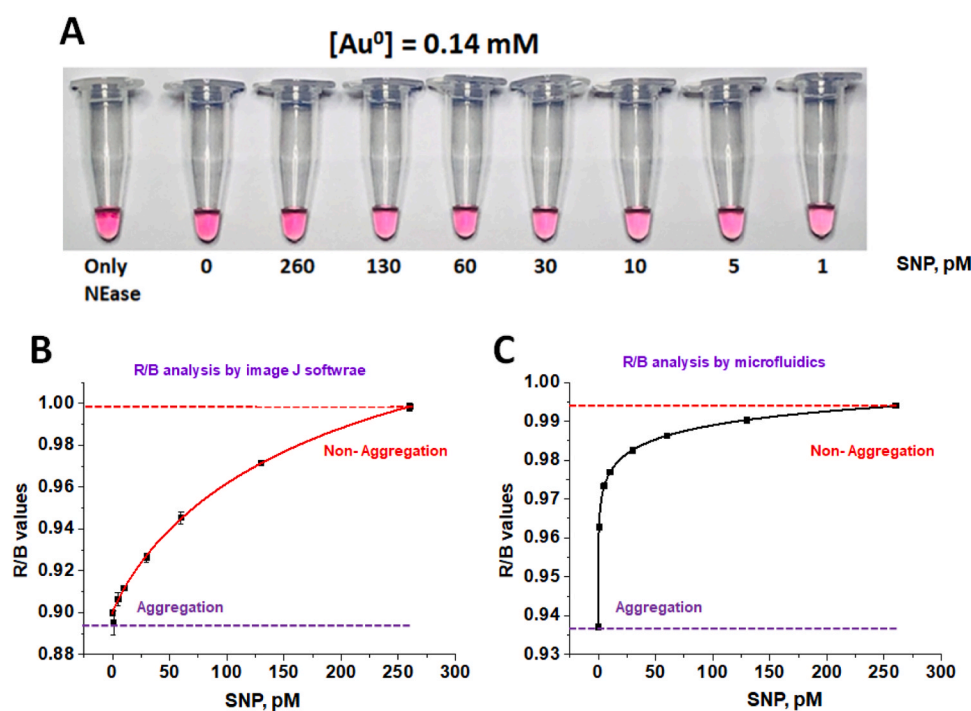
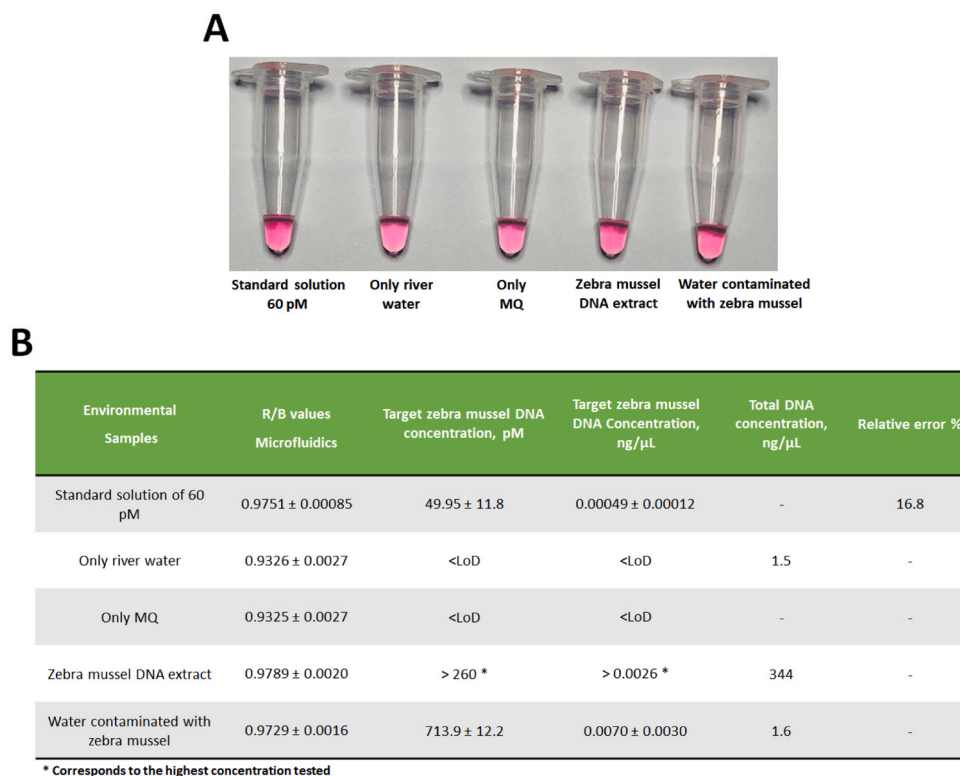


Fig. 5. Colorimetric response analysis of target sequence with one single nucleotide mismatch by A) naked eye visualization, B) RGB analysis by ImageJ software, and C) RGB data obtained by the optical sensor inside the microfluidic system.



**Fig. 6.** Colorimetric response by A) naked eye detection and DNA quantification in environmental samples by B) the RGB sensor.

mixing coil was filled with the carrier and dispensed at the flow rate of 50  $\mu$ L/s, through the mixing coil to the waste, removing the air from the system. Then, the connection tubes between the microtubes with stored solutions and the ports were filled with the respective solutions at a flow rate of 10  $\mu$ L/s.

For a final assessment and further comparison with the previous results, a standard solution of 60 pM was tested. The automated system allowed an automated analysis of the sample within 3 h 10 min, 1.3-fold less time than the standard analysis. The system detected an R/B value of 0.9753  $\pm$  0.0008 and a calculated concentration of 51.9 pM with a relative error of 13.4%, as seen in Table 2. When compared to the approach directly fed into the cartridge and the automated strategy they behaved similarly, indicating the successful application of the automated lab-on-chip DNA amplification and color detection. The lab-on-chip analysis took approximately 3 h and 10 min when compared to the 4 h 30 min for the experiments performed by the user in the lab. Moreover, the automated system only requires the preparation of the solutions to be injected into the system and can run independently without the user's supervision.

The detection of zebra mussels in water samples, found in the literature includes the use of cross-polarized light microscopy (CPLM), scanning electron microscopy (SEM), flow cell cytometry, and polymerase chain reaction (PCR). These approaches have a high cost, are lengthy, and do not allow early detection of this invasive species in the environment. A portable and automated system for in-situ analysis

**Table 2**  
Comparison of direct to automated analysis of samples.

Environmental Samples	R/B values Microfluidics	Target zebra mussel DNA Concentration, pM	Relative error %
*SS of 60 pM – directly	0.8586 $\pm$ 0.0003	49.9	16.8
*SS of 60 pM – Automated	0.8504 $\pm$ 0.0008	51.9	13.4

\* SS- Standard solution

would be a good alternative especially if enables faster analysis time and lower costs [32]. Several researchers have explored automated sample analysis to reduce the need of human intervention, such as pneumatic microfluidic controllers [9]. Additionally, portability is also an important feature, thus research groups have demonstrated ultraportable systems based on isothermal recombinase polymerase amplification for signal amplification [33], smartphone-based platforms integrating Loop-Mediated Isothermal amplification (LAMP) chips for the diagnosis of pathogens [23], multiplexed RT-LAMP assay for human viral disease diagnosis [34], and colorimetric detection of SARS-CoV-2 using a RT-LAMP method within 35 min [35]. However, while LAMP enables portability, it demands high complexity of primer design and the use of multiple primers (inner and outer primers). Other reports such as the detection of SARS-CoV-2 using rt-qPCR have also been used although, this is an expensive technique, and the sample to results time takes 2–48 h [36]. Simpler paper-based microfluidic devices for dengue detection, have also been developed, showing detection limits of  $\sim$ 20 ng mL<sup>-1</sup> for  $\alpha$ -fetoprotein in the serum [37] which is limited when aiming the early detection of zebra mussels for in-situ analysis.

Our system allows running an automated signal amplification and DNA detection, in a single cartridge, within 3 h and 10 min, 1.4-fold faster, than the experimental analysis performed by the user in the lab, which takes 4 h and 30 min. Thus, the system can save up to 1 h 20 min per sample and is compatible with in-situ analysis of environmental samples given its portability. Moreover, the automated system enables the collection of information without the presence of an user.

#### 4. Conclusions

A dual-functional cartridge was developed and used to detect zebra mussel DNA based on enzyme assisted signal amplification and RGB colorimetric detection via an automated and portable system. The detection mode combines AuNP, and signal amplification assisted by NE. The overall system consists of one module integrating a syringe pump for fluidics control and another module integrating a color sensor

with a white led light source and RGB converter, a Peltier for temperature control, and a place to plug the disposable cartridge. Both modules were controlled by homemade software with the option to be run manually or automatically by the user's pre-defined commands. The connection to a laptop is optional. This prototype assembles all the components in a personalized way for suitable analysis on the spot and can be further miniaturized. Two colorimetric detection modes were assessed, naked eye and RGB based on both digital images and converted data by a color sensor. Overall, the colorimetric detection using a large size AuNP of 60 nm compared to 20 nm size enhanced the sensitivity of the system [16]. The LoD for naked eye detection improved from 8 nM to 10 pM whereas for RGB it changed from 0.17 nM to 0.34 pM. The naked eye detection showed detection limitations, especially for the analysis of complex matrices. In general, the two RGB modes tested showed a similar response and allowed specific detection of DNA from zebra mussel. Moreover, the system was also able to discriminate single nucleotide polymorphism (SNP) from fully match DNA even for high concentrations (130 pM). Real samples, zebra mussel meat, and contaminated water with zebra mussel, collected from the Reservoir of La Breña at Guadalquivir, Spain were also successfully analysed. The data obtained on the automated platform with disposable microfluidic cartridges showed good sensitivity and specificity and enable to discriminate single nucleotide polymorphism sensitivity. This system also allowed the successful automated analysis of multiple samples, reducing the analysis time by 1 h and 20 min per sample, taking the technology a step forward in the direction of the miniaturized lab on the chip format, to be used in the field.

#### CRediT authorship contribution statement

The manuscript was written through contributions of all Authors, which also given their approval to the final version. Experiments, characterizations and sample preparation of real samples were conducted by M. Elumalai. Flow cell design and fabrication, as well as microfluidic assembly and software development, were conducted by A. Ipatov. Conceptualization and method development were designed by J. R. Guerreiro and M. Prado. Writing original draft preparation, was conducted by M. Elumalai and J.R. Guerreiro. M. Prado participated on project administration and funding acquisition. Writing—reviewing and editing, was contributed by J.R. Guerreiro, A. Ipatov, M.Elumalai, and M. Prado.

#### Declaration of Competing Interest

The authors declare that they have no known competing financial interests or personal relationships that could have appeared to influence the work reported in this paper.

#### Data Availability

Data will be made available on request.

#### Acknowledgements

The authors thank the Confederación Hidrográfica del Guadalquivir (Spain) for collecting field samples. This work was supported by the Partnership Agreement with Confederación Hidrográfica del Guadalquivir (Spain) for the development of a system of early detection of the zebra mussel through analysis of environmental DNA and by the project Nanotechnology Based Functional Solutions (NORTE-01-0145-FEDER-000019), supported by Norte Portugal Regional Operational Programme (NORTE2020), under the PORTUGAL 2020 Partnership Agreement, through the European Regional Development Fund.

#### Appendix A. Supporting information

Supporting data associated with this article can be found in the online version at [doi:10.1016/j.snb.2023.134722](https://doi.org/10.1016/j.snb.2023.134722).

#### References

- [1] European Parliament, Council of the European Union, REGULATION (EU) No 1143/2014 of the European Parliament and of the Council of 22 October 2014 on the prevention and management of the introduction and spread of invasive alien species, in: *Off. J. Eur. Union*, 2014, 2014, pp. 35–55.
- [2] T. Dejean, A. Valentini, C. Miquel, P. Taberlet, E. Bellemain, C. Miaud, Improved detection of an alien invasive species through environmental DNA barcoding: the example of the American bullfrog *Lithobates catesbeianus*, *J. Appl. Ecol.* 49 (2012) 953–959, <https://doi.org/10.1111/j.1365-2664.2012.02171.x>.
- [3] A. Manz, N. Graber, H.M. Widmer, Miniaturized Total Chemical Analysis Systems: a Novel Concept for Chemical Sensing, 1990.
- [4] G.G. Morbioli, N.C. Speller, M.E. Cato, T.P. Cantrell, A.M. Stockton, Rapid and low-cost development of microfluidic devices using wax printing and microwave treatment, *Sens. Actuators, B Chem.* 284 (2019) 650–656, <https://doi.org/10.1016/j.snb.2018.12.053>.
- [5] N.C. Speller, G.G. Morbioli, M.E. Cato, Z.A. Duca, A.M. Stockton, Green, low-cost, user-friendly, and elastomeric (GLUE) microfluidics, *ACS Appl. Polym. Mater.* 2 (2020) 1345–1355, <https://doi.org/10.1021/acscapm.9b01201>.
- [6] W. Jung, J. Han, J.W. Choi, C.H. Ahn, Point-of-care testing (POCT) diagnostic systems using microfluidic lab-on-a-chip technologies, *Microelectron. Eng.* 132 (2015) 46–57, <https://doi.org/10.1016/j.mee.2014.09.024>.
- [7] B.P. Regmi, M. Agah, Micro gas chromatography: an overview of critical components and their integration, *Anal. Chem.* 90 (2018) 13133–13150, <https://doi.org/10.1021/acs.analchem.8b01461>.
- [8] K. Raj M, S. Chakraborty, PDMS microfluidics: a mini review, *J. Appl. Polym. Sci.* 137 (2020) 1–14, <https://doi.org/10.1002/app.48958>.
- [9] G.G. Morbioli, N.C. Speller, M.E. Cato, A.M. Stockton, An automated low-cost modular hardware and software platform for versatile programmable microfluidic device testing and development, *Sens. Actuators B Chem.* 346 (2021), 130538, <https://doi.org/10.1016/j.snb.2021.130538>.
- [10] N.C. Speller, G.G. Morbioli, M.E. Cato, T.P. Cantrell, E.M. Leydon, B.E. Schmidt, A.M. Stockton, Cutting edge microfluidics: xurography and a microwave, *Sens. Actuators, B Chem.* 291 (2019) 250–256, <https://doi.org/10.1016/j.snb.2019.04.004>.
- [11] J.H. Wang, L.J. Chien, T.M. Hsieh, C.H. Luo, W.P. Chou, P.H. Chen, P.J. Chen, D. S. Lee, G. Bin Lee, A miniaturized quantitative polymerase chain reaction system for DNA amplification and detection, *Sens. Actuators, B Chem.* 141 (2009) 329–337, <https://doi.org/10.1016/j.snb.2009.06.034>.
- [12] S.J. Oh, B.H. Park, G. Choi, J.H. Seo, J.H. Jung, J.S. Choi, D.H. Kim, T.S. Seo, Fully automated and colorimetric foodborne pathogen detection on an integrated centrifugal microfluidic device, *Lab Chip* 16 (2016) 1917–1926, <https://doi.org/10.1039/c6lc00326e>.
- [13] Y. Bai, J. Ji, F. Ji, S. Wu, Y. Tian, B. Jin, Z. Li, Recombinase polymerase amplification integrated with microfluidics for nucleic acid testing at point of care, *Talanta* 240 (2022), 123209, <https://doi.org/10.1016/j.talanta.2022.123209>.
- [14] J. Carvalho, A. Ipatov, L. Rodriguez-Lorenzo, A. Garrido-Maestu, S. Azinheiro, B. Espiña, J. Barros-Velázquez, M. Prado, Towards on-site detection of gluten-containing cereals with a portable and miniaturized prototype combining isothermal DNA amplification and naked eye detection, *Microchem. J.* 183 (2022), <https://doi.org/10.1016/j.microc.2022.108115>.
- [15] D. Vilela, M.C. González, A. Escarpa, Sensing colorimetric approaches based on gold and silver nanoparticles aggregation: chemical creativity behind the assay. A review, *Anal. Chim. Acta* 751 (2012) 24–43, <https://doi.org/10.1016/j.aca.2012.08.043>.
- [16] M. Elumalai, A. Ipatov, J. Carvalho, J. Guerreiro, M. Prado, Dual colorimetric strategy for specific DNA detection by nicking endonuclease-assisted gold nanoparticle signal amplification, *Anal. Bioanal. Chem.* (2021), <https://doi.org/10.1007/s00216-021-03564-5>.
- [17] L. Xu, Y. Zhu, W. Ma, H. Kuang, L. Liu, L. Wang, C. Xu, Sensitive and specific DNA detection based on nicking endonuclease-assisted fluorescence resonance energy transfer amplification, *J. Phys. Chem. C.* 115 (2011) 16315–16321, <https://doi.org/10.1021/jp2036263>.
- [18] S. Yu, S. Chen, Y. Dang, Y. Zhou, J.J. Zhu, An ultrasensitive electrochemical biosensor integrated by nicking endonuclease-assisted primer exchange reaction cascade amplification and DNA Nanosphere-mediated Electrochemical Signal-enhanced System for MicrorRNA Detection, *Anal. Chem.* 94 (2022) 14349–14357, <https://doi.org/10.1021/acs.analchem.2c03015>.
- [19] L.A. Dauphin, B.D. Moser, M.D. Bowen, Evaluation of five commercial nucleic acid extraction kits for their ability to inactivate *Bacillus anthracis* spores and comparison of DNA yields from spores and spiked environmental samples, *J. Microbiol. Methods* 76 (2009) 30–37, <https://doi.org/10.1016/j.mimet.2008.09.004>.
- [20] W. Xu, X. Xue, T. Li, H. Zeng, X. Liu, Ultrasensitive and selective colorimetric dna detection by nicking endonuclease assisted. Nanoparticle amplification, *Angew. Chem. - Int. Ed.* 48 (2009) 6849–6852, <https://doi.org/10.1002/anie.200901772>.
- [21] T.T. Wang, C. kit Lio, H. Huang, R.Y. Wang, H. Zhou, P. Luo, L. Sen Qing, A feasible image-based colorimetric assay using a smartphone RGB camera for point-of-care

- monitoring of diabetes, *Talanta* 206 (2020), 120211, <https://doi.org/10.1016/j.talanta.2019.120211>.
- [22] Q. Wei, R. Nagi, K. Sadeghi, S. Feng, E. Yan, S.J. Ki, R. Caire, D. Tseng, A. Ozcan, Detection and spatial mapping of mercury contamination in water samples using a smart-phone, *ACS Nano* 8 (2014) 1121–1129, <https://doi.org/10.1021/nl406571t>.
- [23] H.Q. Nguyen, V.D. Nguyen, H. Van Nguyen, T.S. Seo, Quantification of colorimetric isothermal amplification on the smartphone and its open-source app for point-of-care pathogen detection, *Sci. Rep.* 10 (2020) 1–10, <https://doi.org/10.1038/s41598-020-72095-3>.
- [24] S. Kim, J. De Jonghe, A.B. Kulesa, D. Feldman, T. Vatanen, R.P. Bhattacharyya, B. Berdy, J. Gomez, J. Nolan, S. Epstein, P.C. Blainey, High-throughput automated microfluidic sample preparation for accurate microbial genomics, *Nat. Commun.* 8 (2017), <https://doi.org/10.1038/ncomms13919>.
- [25] P.U. Alves, R. Vinhas, A.R. Fernandes, S.Z. Birol, L. Trabzon, I. Bernacka-Wojcik, R. Igreja, P. Lopes, P.V. Baptista, H. Águas, E. Fortunato, R. Martins, Multifunctional microfluidic chip for optical nanoprobe based RNA detection - application to chronic myeloid leukemia, *Sci. Rep.* 8 (2018) 1–10, <https://doi.org/10.1038/s41598-017-18725-9>.
- [26] K.R. Brown, D.G. Walter, M.J. Natan, Seeding of colloidal Au nanoparticle solutions. 2, Improved control of particle size and shape, *Chem. Mater.* (2000) 306–313, <https://doi.org/10.1021/cm980065p>.
- [27] M. Sanromán-Iglesias, C.H. Lawrie, T. Schäfer, M. Grzelczak, L.M. Liz-Marzán, Sensitivity limit of nanoparticle biosensors in the discrimination of single nucleotide polymorphism, *ACS Sens.* 1 (2016) 1110–1116, <https://doi.org/10.1021/acssensors.6b00393>.
- [28] P.K. Jain, K.S. Lee, I.H. El-Sayed, M.A. El-Sayed, Calculated absorption and scattering properties of gold nanoparticles of different size, shape, and composition: applications in biological imaging and biomedicine, *J. Phys. Chem. B* 110 (2006) 7238–7248, <https://doi.org/10.1021/jp057170o>.
- [29] S.J. Hurst, H.D. Hill, C.A. Mirkin, “Three-dimensional hybridization” with polyvalent DNA-gold nanoparticle conjugates, *J. Am. Chem. Soc.* 130 (2008) 12192–12200, <https://doi.org/10.1021/ja804266j>.
- [30] K. Yin, V. Pandian, K. Kadimisetty, X. Zhang, C. Ruiz, K. Cooper, C. Liu, Real-time colorimetric quantitative molecular detection of infectious diseases on smartphone-based diagnostic platform, *Sci. Rep.* 10 (2020) 1–9, <https://doi.org/10.1038/s41598-020-65899-w>.
- [31] H.C. Zec, T. Zheng, L. Liu, K. Hsieh, T.D. Rane, T. Pederson, T.-H. Wang, Programmable microfluidic genotyping of plant DNA samples for marker-assisted selection, *Microsyst. Nanoeng.* 4 (2018) 1–10, <https://doi.org/10.1038/micronano.2017.97>.
- [32] D.M. Hosler, Early detection of dreissenid species: Zebra/Quagga mussels in water systems, *Aquat. Invasions* 6 (2011) 217–222, <https://doi.org/10.3391/ai.2011.6.2.10>.
- [33] H. Xu, A. Xia, D. Wang, Y. Zhang, S. Deng, W. Lu, J. Luo, Q. Zhong, F. Zhang, L. Zhou, W. Zhang, Y. Wang, C. Yang, K. Chang, W. Fu, J. Cui, M. Gan, D. Luo, M. Chen, An ultraportable and versatile point-of-care DNA testing platform, *Sci. Adv.* 6 (2020), <https://doi.org/10.1126/sciadv.aaz7445>.
- [34] D. Natsuhara, R. Saito, H. Aonuma, T. Sakurai, S. Okamoto, M. Nagai, H. Kanuka, T. Shibata, A method of sequential liquid dispensing for the multiplexed genetic diagnosis of viral infections in a microfluidic device, *Lab Chip* 21 (2021) 4779–4790, <https://doi.org/10.1039/d1lc00829c>.
- [35] M.N. Aoki, B. de Oliveira Coelho, L.G.B. Góes, P. Minoprio, E.L. Durigon, L. G. Morello, F.K. Marchini, I.N. Riediger, M. do Carmo Debur, H.I. Nakaya, L. Blanes, Colorimetric RT-LAMP SARS-CoV-2 diagnostic sensitivity relies on color interpretation and viral load, *Sci. Rep.* 11 (2021) 1–10, <https://doi.org/10.1038/s41598-021-88506-y>.
- [36] C.B.F. Vogels, A.F. Brito, A.L. Wyllie, J.R. Fauver, I.M. Ott, C.C. Kalinich, M. E. Petrone, A. Casanovas-Massana, M. Catherine Muenker, A.J. Moore, J. Klein, P. Lu, A. Lu-Culligan, X. Jiang, D.J. Kim, E. Kudo, T. Mao, M. Moriyama, J.E. Oh, A. Park, J. Silva, E. Song, T. Takahashi, M. Taura, M. Tokuyama, A. Venkataraman, O. El Weizman, P. Wong, Y. Yang, N.R. Cheemarla, E.B. White, S. Lapidus, R. Earnest, B. Geng, P. Vijayakumar, C. Odio, J. Fournier, S. Bermejo, S. Farhadian, C.S. Dela Cruz, A. Iwasaki, A.I. Ko, M.L. Landry, E.F. Foxman, N.D. Grubaugh, Analytical sensitivity and efficiency comparisons of SARS-CoV-2 RT-qPCR primer-probe sets, *Nat. Microbiol.* 5 (2020) 1299–1305, <https://doi.org/10.1038/s41564-020-0761-6>.
- [37] Y. Zhang, J. Bai, J.Y. Ying, A stacking flow immunoassay for the detection of dengue-specific immunoglobulins in salivary fluid, *Lab Chip* 15 (2015) 1465–1471, <https://doi.org/10.1039/c4lc01127a>.

**Monisha Elumalai** is currently a Postdoctoral Researcher at Purdue University Weldon School of Biomedical Engineering (USA). She holds a PhD in the science and technology of colloids and interfaces from University of Vigo (Spain) and in collaboration with the International Iberian Nanotechnology Laboratory (Portugal). She did her Master of Technology in the field of sensor system technology (India) and Bachelor of Engineering in the field of electronics and communication engineering (India). Her research interests focus on the development of optical biosensors, nanoparticle synthesis and characterization, DNA functionalization on nanoparticles, DNA amplification techniques, developing automated microfluidic systems, design of paper fluidic devices, developing point-of-care devices, and gas sensors.

**Andrey Ipatov** is a Research Engineer in the food quality and safety group at International Nanotechnology Laboratory (INL). He received his PhD in natural science from Roskilde University (Denmark) with a focus on the multisensor detection of multicomponent liquids. His postdoctoral research at the Institute of the Microelectronics of Barcelona (2005–2014) was devoted to the study of ISFETs for multicomponent detection in natural and artificial liquids. He has a background in analytical chemistry, modeling, design, and fabrication of microfluidic devices and sensor integration. He is currently involved in projects which aim to develop microfluidic devices for the extraction, amplification, and detection of environmental DNA. Particularly, he designs and fabricates microfluidic cell components with a CNC milling machine, laser cutter, and other techniques. His scientific interests also include flow injection analysis, electrochemical and optical sensors, chemometrics, sensor array, development of new analytical methods, and portable systems for analysis of liquids. He is an expert on miniaturization and integration of analytical devices to produce POC devices.

**Joana Guerreiro** holds a Research Position at the Centre of Biological Engineering – University of Minho and BioMark Sensor Research – ISEP, since 2021. She received her PhD in chemistry (2015) from the University of Porto, Portugal, in straight collaboration with Aarhus University, Denmark. Afterward, she worked as Postdoctoral Researcher at iNANO (Denmark) for one year and at International Iberian Nanotechnology Laboratory (Portugal) for four years. She has been working on the biosensing field and on the development of new sensing materials for more than 13 years. Her main research interests focus on the development of optical biosensors, synthesis of metallic nanostructures, design of microfluidic systems, and paper-based devices for the detection of target analytes (biomarkers, DNA), applied to the health and environmental fields.

**Marta Prado** is Group Leader of the Food Quality and Safety Research Group (FQ&S) and the Food Cluster Coordinator at the International Iberian Nanotechnology Laboratory (INL). Her research interests are the development of new, fast, and reliable detection methodologies combining molecular biology, nano and microfabrication for different applications for food safety and quality, working in both targeted and non-targeted methods. She has a PhD in food science and technology from the University of Santiago de Compostela (Spain) and she worked at the Joint Research Center from the European Commission (JRC-EC) in Geel (Belgium) as Scientific Officer between 2005 and 2010. In 2010, she moved to INL where she currently leads a team of researchers.